Oxomanganese(IV) Porphyrins Identified by Resonance Raman and Infrared Spectroscopy: Weak Bonds and the Stability of the Half-Filled t_{2g} Subshell

Roman S. Czernuszewicz, Y. Oliver Su,† Michael K. Stern, Kathleen A. Macor, Dongho Kim, John T. Groves,* and Thomas G. Spiro*

Contribution from the Department of Chemistry, Princeton University, Princeton, New Jersey 08544. *Received August 27, 1987*

Abstract: The Mn^{IV}-O stretching frequency is identified at 754 cm^{-1} in resonance Raman (RR) and infrared (IR) spectra of Mn^{IV} porphyrins prepared by electrooxidation of $ClMn^{III}TMP$ (TMP = tetramesitylporphyrin), $ClMn^{III}TPP$ (TPP = tetraphenylporphyrin) and $ClMn^{III}OEP$ (OEP = octaethylporphyrin) in CH_3CN containing tetrabutylammonium hydroxide (TBA(OH)). This vibrational band establishes oxo-Mn^{IV} bond formation under these conditions and shows the bond to be anomalously weak. When the oxidation is carried out in CH_2Cl_2 containing TBA(OH), or when $ClMn^{III}TMPyP$ (TMPyP = tetrakis(methylpyridinium)porphyrin) is electrooxidized in aqueous 1 M NaOH, the Mn-O stretching band is seen at 711 cm^{-1}. This band is associated with a trans OH^- adduct, as shown by its anomalous upshift, to 732 cm^{-1}, in D_2O; the lower frequency in H_2O is attributed to interaction with the Mn-O-H bend of the trans OH^- ligand, which is relieved when H is replaced by D. EPR spectra of all these species show strong $g_\perp \sim 4.0$ and weak $g_\parallel \sim 2.0$ signals characteristic of a high-spin d^3 configuration. The $Mn^{III}TMPyP$ species in 1 M NaOH is shown to be a trans dihydroxide adduct by virtue of a 495-cm^{-1} RR band identified, on the basis of its $H_2{}^{18}O$ and D_2O shifts, as the symmetric Mn-$(OH)_2$ stretch. The M-O stretching frequencies are compared for V^{IV}, Cr^{IV}, Mn^{IV}, and Fe^{IV} porphyrins, and the anomalous weakness of the Mn^{IV}-O bond is attributed to the special stability and low polarizability of the half-filled t_{2g}^3 subshell. Consequences of this weak bond for manganyl reactivity are discussed.

It is now well appreciated that the formation of oxoiron(IV) porphyrin species is central to the strategies of biological dioxygen reduction. The characterization of the celebrated compounds I and II of horseradish peroxidase,[1] as well as synthetic iron porphyrin models for each,[2] has established a low-spin d^4 electronic configuration[2c,3] for the ferryl moiety [Fe=O] and a relatively short iron-oxygen bond.[4] Similar formulations have been proposed for cytochrome *c* peroxidase compound ES[5] and for the as yet unseen active oxygen species of cytochrome P-450.[6] Moreover, biomimetic model systems for these heme proteins have been described which involve oxometalloporphyrin complexes of chromium,[7] manganese,[8] and ruthenium.[9] Oxo complexes of titanium,[10] vanadium,[11] molybdenum,[12] niobium,[13] osmium,[14] and rhenium[11b] have also been reported.

Among the well characterized oxo complexes of this type the oxoiron(IV) species stand alone as representatives of the class of oxo complexes with populated M=O π-antibonding orbitals. An isoelectronic oxoruthenium(IV) porphyrin complex has also recently been described.[9c] Manganese(IV) porphyrins recently isolated and characterized in our laboratories[8b] and elsewhere[8e] have been suggested on the basis of chemical reactivity and spectral properties to be the first manganyl porphyrins.[8b] The expected high-spin d^3 electronic configuration of such species would provide an important point of comparison for the closely related iron case.

The most direct evidence for oxo-metal bonds comes from Raman or infrared spectroscopy, in which the M-O stretching vibration can be revealed by its characteristic mass dependence upon $^{18/16}O$ substitution. A recent spate of reports[15] reveal the Fe^{IV}=O stretch of ferryl porphyrins to be in the ~800-cm^{-1} region; the systematics of these frequencies are discussed in the preceding article. No comparable evidence for M^{IV}=O bonds has hitherto been described. Indeed a recent resonance Raman (RR) spectroscopic study[15k] of compound II of Mn-substituted HRP revealed an ^{18}O-sensitive band (620 cm^{-1}) which was assigned to Mn^{IV}—OH rather than Mn^{IV}=O stretching, because it shifts down 18 cm^{-1} in D_2O, as expected from the OD mass effect. This observation suggests that the putative Mn^{IV}=O bond has a high proton affinity and raises the possibility that it might be too basic to observe under normal conditions.

* Authors to whom correspondence should be addressed.
† Present address: Department of Chemistry, National Taiwan University, Taipei, Taiwan, Republic of China.

(1) (a) Dunford, H. B.; Stillman, J. S. *Coord. Chem. Rev.* **1976**, *19*, 187-251. (b) Hewson, W. D.; Hager, L. P. In *The Porphyrins*: Dolphin, D., Ed.; Academic: New York, 1979; Vol. 7, pp 295-332. (c) Frew, J. E.; Jones, P. *Adv. Inorg. Bioinorg. Mech.* **1984**, *3*, 175-212. (d) Yonetani, T.; Yamamoto, H.; Erman, J. E.; Leigh, J. S.; Reed, G. H. *J. Biol. Chem.* **1971**, *247*, 2447-2455. (e) Mauk, M. R.; Girotii, A. W. *Biochemistry* **1974**, *13*, 1757-1763.

(2) (a) Groves, J. T.; Haushaulter, R. C.; Nakamura, M.; Nemo, T. E.; Evans, B. J. *J. Am. Chem. Soc.* **1981**, *103*, 2884-2886. (b) Groves, J. T.; Quinn, R.; McMurry, T. J.; Lang, G.; Boso, B. *J. Chem. Soc., Chem. Commun.* **1984**, 1455-1456. (c) Chin, D. H.; Balch, A. L.; La Mar, G. N. *J. Am. Chem. Soc.* **1980**, *102*, 1446-1448. (d) Chin, D. H.; La Mar, G. N.; Balch, A. L. *J. Am. Chem. Soc.* **1980**, *102*, 4344-4350. (e) Balch, A. L.; La Mar, G. N.; Latos-Grazynski, L.; Renner, M. W.; Thanabal, V. *J. Am. Chem. Soc.* **1985**, *107*, 3003-3007.

(3) (a) Boso, B.; Lang, G.; McMurry, T. J.; Groves, J. T. *J. Chem. Phys.* **1983**, *79*, 1122-1126. (b) La Mar, G. N.; de Ropp, J. S.; Smith, K. M.; Langry, K. C. *J. Biol. Chem.* **1981**, *256*, 237-243.

(4) (a) Penner-Hahn, J. E.; McMurry, T. J.; Renner, M.; Latos-Grazynsky, L.; Eble, K. S.; Davis, I. M.; Balch, A. L.; Groves, J. T.; Dawson, J. R.; Hodgson, K. O. *J. Biol. Chem.* **1983**, *258*, 12761-12764. (b) Penner-Hahn, J. E.; Eble, K. S.; McMurry, T. J.; Renner, M.; Balch, A. L.; Groves, J. T.; Dawson, J. R.; Hodgson, K. O. *J. Am. Chem. Soc.* **1986**, *108*, 7819-7825.

(5) (a) Hori, H.; Yonetani, T. *J. Biol. Chem.* **1985**, *260*, 349-355. (b) Poulos, T. L.; Kraut, J. *J. Biol. Chem.* **1980**, *255*, 8199-8205. (c) Poulos, T. L.; Freer, S. T.; Alden, R. A.; Edwards, S. L.; Skogland, U.; Takio, K.; Eriksson, B.; Xuong, N.; Yonetani, T.; Kraut, J. *J. Biol. Chem.* **1980**, *255*, 575-580. (d) Tahio, K.; Titani, K.; Ericson, L. H.; Yonetani, T. *Arch. Biochem. Biophys.* **1980**, *203*, 615-629.

(6) (a) Sligar, S. G.; Murray, R. I. *Cytochrome P-450 Structure, Mechanism, and Biochemistry*; Oritz de Montellano, P. R., Ed.; Plenum: New York, 1986; pp 443-479. (b) Guengerich, F. P.; MacDonald, T. L. *Acc. Chem. Res.* **1984**, *17*, 9-16. (c) White, R. E.; Coon, M. J. *Annu. Rev. Biochem.* **1980**, *49*, 315-336. (d) Groves, J. T. *Adv. Inorg. Biochem.* **1979**, 119-145.

(7) (a) Groves, J. T.; Kruper, W. J. *J. Am. Chem. Soc.* **1979**, *101*, 7613-7615. (b) Groves, J. T.; Haushalter, R. C. *J. Chem. Soc., Chem. Commun.* **1981**, 1163-1166. (c) Groves, J. T.; Kruper, W. J., Jr.; Haushalter, R. C.; Butler, W. M. *Inorg. Chem.* **1982**, *21*, 1363-1368. (d) Penner-Hahn, J. E.; Benfatto, M.; Hedman, B.; Takahashi, T.; Sebastian, D.; Groves, J. T.; Hodgson, K. O. *Inorg. Chem.* **1986**, *25*, 2255-2259.

(8) (a) Groves, J. T.; Watanabe, Y.; McMurry, T. J. *J. Am. Chem. Soc.* **1983**, *105*, 4489-4490. (b) Groves, J. T.; Stern, M. K. *J. Am. Chem. Soc.* **1987**, *109*, 3812-3814. (c) Bortoloni, O.; Meunier, B. *J. Chem. Soc., Chem. Commun.* **1983**, 1364. (d) Bortoloni, O.; Ricci, M.; Meunier, B.; Friant, P.; Ascone, I.; Goulon, J. *Nouv. J. Chim.* **1986**, *10*, 39-49. (e) Schappacher, M.; Weiss, R. *Inorg. Chem.* **1987**, *26*, 1190-1192.

0002-7863/88/1510-4158$01.50/0

We now report the first identification of the Mn=O bond, formed by oxidation of Mn^{III} porphyrins in hydroxide-containing media, using RR and IR spectroscopy. The RR technique has proven to be especially useful since the Mn^{IV}=O stretch is enhanced in resonance with the porphyrin electronic transitions. The frquencies are the lowest yet reported for oxo–metal bonds. When compared to other five-coordinate ($M^{IV}O$) porphyrin species, the M–O stretching frequency for Mn is ~100 cm^{-1} lower than for Fe, and ~250 cm^{-1} lower than for V and Cr, even though Mn occupies an intermediate position in this series. The anomaly is attributable to the special stability of the half-filled t_{2g} subshell which comes into play for the d^3 configuration of Mn^{IV}. The result is a high-spin configuration, confirmed by EPR spectroscopy, with the same M=O bond order as for (low-spin) Fe^{IV}=O. The extra lowering of the Mn^{IV}=O stretching frequency is attributable to the contraction of the d orbitals in the half-filled shell, which reduces their availability for π bonding.

Materials and Methods

Benzene and acetonitrile were purified by standard methods and distilled from $LiAlH_4$ and CaH_2, respectively. Dichloromethane was freshly distilled from CaH_2 prior to each use. Tetrabutylammonium perchlorate (TBAP) (GFS Chemicals, Columbus, OH) was recrystallized three times from ethanol and dried in vacuo overnight. Tetramethyl- and tetrabutylammonium (TBA(OH)) hydroxides were purchased from Aldrich Chemical Co. (Milwaukee, WI) and were used as received.

Manganese(III) complexes of octaethylporphyrin (OEP), tetraphenylporphyrin (TPP), and tetrakis(methylpyridinium)porphyrin (TMPyP) were purchased from Mid Century Chemicals (Posen, IL) and were used without any further purification. Tetramesitylporphyrin (TMP) was prepared by the method of Badger et al.,[16] with modifications as described in ref 17. Metalation to $ClMn^{III}TMP$ (**1**) was achieved following the literature method.[18]

UV–vis Absorption Spectroscopy and Electrochemistry. Electronic absorption spectra were measured on Cary 2390 or IBM 9430 spectrophotometers.

Controlled-potential electrolysis and thin-layer spectroelectrochemistry of TMP species were carried out in CH_2Cl_2 or CH_3CN with TBAP (0.1 M) as supporting electrolyte with use of a BAS 100 electrochemical analyzer and a BAS SP-2 potentiostat. The bulk electrolysis cell was equipped with reticulated vitreous carbon (RVC) working, Pt wire auxiliary, and Hg/HgO (0.1 M NaOH) reference electrodes. Thin-layer spectroelectrochemistry was performed in a homemade quartz cell with optically transparent RVC working, Pt wire auxiliary, and Hg/HgO reference electrodes.

Cyclic voltammetry, controlled-potential electrolysis, and thin-layer spectroelectrochemistry of TMPyP species were carried out in 1 M NaOH aqueous solution, using glassy carbon or Pt mesh working electrodes. A Pt wire served as an auxiliary electrode, and all potentials were measured versus a saturated calomel (SCE) reference electrode.

(a) Generation of $ClMn^{III}TMP^{\cdot+}$ π-Cation Radical. A 6-mL portion of a CH_2Cl_2 stock $ClMn^{III}TMP$ (**1**) solution (2.3 μM) containing TBAP as supporting electrolyte (0.1 M) was cooled to −20 °C in an electrochemical cell. A potential of +1.2 V was applied to the cell for 15 min resulting in the formation of a new species, **4**, with a characteristic π-cation radical visible spectrum[8d,19] (λ_{max} = 380, 478, and 620 nm). A 3-mL portion of the oxidized solution was transferred to a quartz cuvette, maintained at −20 °C in the thermostated sample compartment of a Cary 2390 spectrometer, and spectrophotometrically titrated by adding tetrabutylammonium iodide (TBA(I)) in 0.25-equiv aliquots. A total of 1 equiv of TBA(I) was required to completely convert **4** to Mn(III) porphyrin complex.

(b) Ligand Metathesis of 4 to Oxo-$Mn^{IV}TMP$[3]. Addition to 20 μL of a TBA(OH) solution (40% in H_2O) in a 3-mL aliquot of **4**, generated at −20 °C as described above, caused an immediate color change from green to red. The resulting visible spectrum was characteristic of a stable oxo-$Mn^{IV}TMP$ complex **3** (λ_{max} = 425, 470, 513, 562, 621, 654 nm).

(c) Generation of Oxo-$Mn^{IV}TMP$[5] in CH_3CN. **1** (0.25 mg, 0.28 μmol) was dissolved in 10 mL of CH_3CN containing 0.1 M TBAP. TBA(OH) (5 μL) was added and the solution was oxidized at +0.6 V in a bulk electrolysis cell with a RVC working electrode. The electrolysis was complete within 5 min, resulting in a stable red species (λ_{max} = 418, 460, 492, 536, and 580 nm).

(d) Thin-Layer Spectroelectrochemistry. Reduction and reoxidation of oxo-$Mn^{IV}TMP$ complex **2** was performed in the following manner. $ClMn^{III}TMP$ (0.7 mg, 0.80 μmol) was dissolved at 0 °C in 5 mL of CH_2Cl_2/0.1 M TBAP. Addition of 2.0 equiv of $(CH_3)_4NOH$ (10.29 mg, 1.6 μmol) followed by 1.2 equiv of *m*-chloroperoxybenzoic acid (mCPBA) (10.16 mg, 0.96 μmol) resulted in the generation of **2**. The solution was transferred to a quartz spectroelectrochemical cell. At a voltage of +0.1 V **2** was cleanly reduced, generating a Mn(III) porphyrin visible spectrum. Reoxidation at +0.9 V resulted in the isosbestic generation of the visible spectrum of **2**. This reduction/oxidation process was cycled several times without any detectable porphyrin decomposition.

The spectroelectrochemical reversible oxidation of $(AcO)Mn^{III}TMPyP$ was performed in a quartz cuvette cell equipped with a Pt mesh working electrode, a Pt wire auxiliary electrode, and a SCE reference electrode. The sample solutions were prepared by dissolving $(AcO)Mn^{III}TMPyP$ in 1 M NaOH solution (pH 14).

Infrared Spectroscopy. Infrared (IR) spectra were measured in KBr pellets on a Nicolet 5DBX fourier-transform IR spectrometer.

A solid sample of oxo-$Mn^{IV}TMP$ complex **2** was isolated as previously described.[8b]

(a) Conversion of 2 to 3 by Addition of TBA(OH). A sample of **1** (13.0 mg, 14.9 μmol) was dissolved in 1 mL of CH_2Cl_2, and the solution was cooled to 0 °C. Addition of $(CH_3)_4NOH$ (2.0 equiv, 5.4 mg in 10 μL of MeOH) and *m*-CPBA (1.2 equiv, 3.0 mg) caused an immediate color change from green to red. TBA(OH) (100 μL, 40% in H_2O) was added and the solution was allowed to stir for 3 min. The resulting complex **3** was isolated by low-temperature (−78 °C) alumina chromatography as previously described.[8b] Preparation of the KBr pellets caused no appreciable decompositioin of **2** or **3** as determined by visible spectroscopy.

EPR Spectroscopy. The EPR spectra were recorded on a Varian E-12 spectrometer at 120 K.

A sample of oxo-$Mn^{IV}TMP$ complex **5** suitable for EPR analysis was prepared by dissolving **1** (24.5 mg, 28.1 μmol) in 10 mL of CH_3CN containing 150 μL of TBA(OH) (40% in H_2O). The solution was oxidized at +0.7 V in the bulk electrolysis cell until it was determined by visible spectroscopy to be 100% Mn^{IV} species. A portion of this solution was then transferred to an EPR tube and immediately frozen in liquid N_2.

The $(HO-Mn^{IV}O)TMPyP$ complex, **6**, was generated by electrooxidation of $(AcO)Mn^{III}TMPyP$ (5 mM) at +0.30 V in 1 M NaOH solution.

(9) (a) Groves, J. T.; Quinn, R. *Inorg. Chem.* **1984**, *23*, 3846–3853. (b) Groves, J. T.; Quinn, R. *J. Am. Chem. Soc.* **1985**, *107*, 5790–5792. (c) Groves, J. T.; Ahn, K.-H. *Inorg. Chem.* **1987**, *26*, 3831–3833.

(10) (a) Latour, J. M.; Gallund, B.; Marchon, J.-L. *J. Chem. Soc., Chem. Commun.* **1979**, 570. (b) Eaton, S. S.; Eaton, G. R. *J. Am. Chem. Soc.* **1975**, *97*, 3660.

(11) (a) Pattersen, R. C.; Alexander, L. E. *J. Am. Chem. Soc.* **1968**, *90*, 3873–3875. (b) Buchler, J. W.; Puppe, L.; Rohbock, K.; Schneehage, H. M. *Ann. N.Y. Acad. Sci.* **1973**, *206*, 116. (c) Kadish, K. M.; Morrison, M. M. *Bioinorg. Chem.* **1977**, *7*, 107–115.

(12) (a) Diebold, T.; Chevrier, B.; Weiss, R. *Inorg. Chem.* **1979**, *18*, 1193. (b) Ledon, H.; Mentzen, B. *Inorg. Chim. Acta* **1978**, *31*, L393.

(13) (a) Matsuda, Y.; Sakamoto, S.; Koshima, H.; Murakami, Y. *J. Am. Chem. Soc.* **1985**, *107*, 6415–6416. (b) Matsuda, Y.; Yamada, S.; Goto, T.; Murakami, Y. *Bull. Chem. Soc. Jpn.* **1981**, *54*, 452–457.

(14) Buchler, J. W.; Smith, P. D. *Angew. Chem., Int. Ed. Engl.* **1974**, *13*, 341.

(15) (a) Terner, J.; Sitter, A. J.; Reczek, C. M. *Biochem. Biophys. Acta* **1985**, *828*, 73–80. (b) Hashimoto, S.; Tatsuno, Y.; Kitagawa, T. *Proc. Jpn. Acad. Ser. B* **1984**, *60*, 345–348. (c) Sitter, A. J.; Reczek, C. M.; Terner, J. *J. Biol. Chem.* **1985**, *260*, 7515–7522. (d) Hashimoto, S.; Teraoka, J.; Inubushi, T.; Yonetani, T.; Kitagawa, T. *J. Biol. Chem.* **1986**, *261*, 11110–11118. (e) Hashimoto, S.; Tatsuno, Y.; Kitagawa, T. *Proc. Natl. Acad. Sci. U.S.A.* **1986**, *83*, 2417–2421. (f) Sitter, A. J.; Reczek, C. M.; Terner, J. *Biochem. Biophys. Acta* **1985**, *828*, 229–235. (g) Bajdor, K.; Nakamoto, K. *J. Am. Chem. Soc.* **1984**, *106*, 3045–3046. (h) Proniewicz, L. M.; Bajdor, K.; Nakamoto, K. *J. Phys. Chem.* **1986**, *90*, 1760–1766. (i) Schappacher, M.; Chottard, G.; Weiss, R. *J. Chem. Soc., Chem. Commun.* **1986**, *2*, 93–94. (j) Sitter, A. J.; Reczek, C. M.; Terner, J. *J. Biol. Chem.* **1986**, *261*, 8638–8642. (k) Makino, R.; Uno, T.; Nishimura, Y.; Iizuka, T.; Tsuboi, M.; Ishimura, Y. *J. Biol. Chem.* **1986**, *261*, 8376–8382. (l) Hashimoto, J.; Tatauno, Y.; Kitagawa, T. In *Proceedings of the Tenth International Conference on Raman Spectroscopy*; Peticolas, W. L., Hudson, B., Eds.; University of Oregon, Eugene, OR; pp 1–29. (m) Kean, R. T.; Oertling, W. A.; Babcock, G. T. *J. Am. Chem. Soc.* **1987**, *109*, 2185–2187.

(16) Badger, G. M.; Jones, R. A.; Laslett, R. L. *Aust. J. Chem.* **1964**, *17*, 1028–1035.

(17) Groves, J. T.; Nemo, T. E. *J. Am. Chem. Soc.* **1983**, *105*, 5786–5791.

(18) Kruper, W. J. Ph.D. Thesis, The University of Michigan, 1982.

(19) (a) Spreer, L. O.; Maliyackel, A. C.; Holbrook, S.; Otvos, J. W.; Calvin, M. *J. Am. Chem. Soc.* **1986**, *108*, 1949–1953. (b) Carnieri, N.; Harriman, A.; Porter, G.; Kalyanasundaram, K. *J. Chem. Soc., Dalton Trans.* **1982**, 1231. (c) Phillippi, M. A.; Shinomura, E. T.; Goff, H. M. *Inorg. Chem.* **1981**, *20*, 1322.

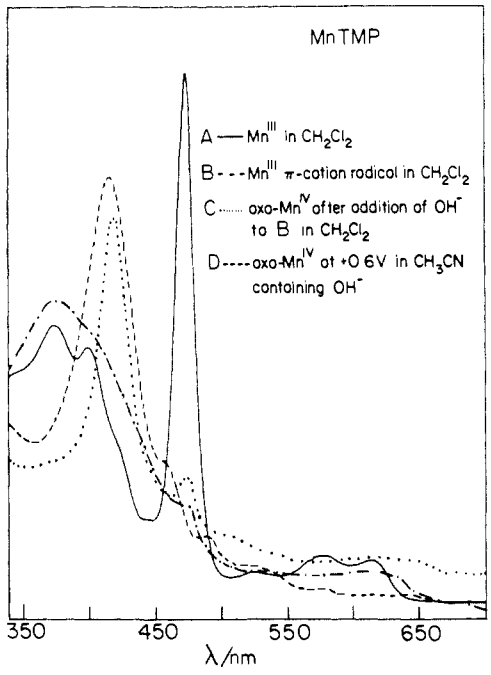

Figure 1. Electronic absorption spectra of MnTMP porphyrins: (A) —, $ClMn^{III}TMP$ (**1**) in CH_2Cl_2 (λ_{max} = 372, 401, 478, 586, 620 mm); (B) - - -, $ClMn^{III}TMP$ π-cation radical (**4**) generated at −20 °C by electrochemical oxidation of **1** in CH_2Cl_2 (0.1 M TBAP) at +1.2 V (λ_{max} = 380, 478, 620 nm); (C) ···, $(Mn^{IV}O)TMP$ (**3**) after reaction of a CH_2Cl_2 solution of **4**, with TBA(OH) (λ_{max} = 425, 470, 513, 562, 621 nm); (D) - - -, $(Mn^{IV}O)TMP$ (**5**) generated by electrochemical oxidation of **1**, in CH_3CN (0.1 M TBAP) containing TBA(OH) at +0.6 V (λ_{max} = 418, 460 sh, 492, 533, 580 nm).

Resonance Raman Spectroscopy. A three-electrode bulk electrolysis Raman cell,[20] with Pt gauze working electrode, saturated calomel (SCE) electrode, and Pt wire auxiliary electrode, was used for oxidation of Mn(III) porphyrins. The design of the cell allowed for Raman spectra to be recorded in situ in backscattering geometry. Mn(III) complexes of TMP, TPP, and OEP were oxidized in CH_3CN containing 0.04 M TBA(OH) and 0.1 M TBAP as a supporting electrolyte. Isotopically enriched TBA(OH) were prepared by exchange of $H_2{}^{18}O$ (98% ^{18}O, Cambridge Isotopes) or D_2O with a 40% TBA(OH) aqueous solution. Typically 100 μL of TBA(OH) was placed under vacuum until solid began to form. The solid material was redissolved in 100 μL of the appropriate isotopically enriched H_2O and then the solution was evaporated again. This procedure was repeated three times. The Mn^{III} complex of TMPyP was oxidized in 1 M $NaOH/H_2O$ or 1 M $NaOD/D_2O$ solution. The ^{18}O Raman shift was determined from a sample oxidized chemically with potassium ferricyanide in 1 M NaOH $H_2{}^{18}O$ solution. For these measurements Raman spectra were obtained via backscattering from a spinning NMR tube.

Exciting radiation for RR spectra was provided by Spectra Physics 171 Kr^+ (4067 Å) and Spectra Physics 2020 Ar^+ (4579 Å) ion lasers. The scattered radiation was dispersed by a Spex 1401 double monochromator and detected by a cooled RCA 31034A photomultiplier tube with an ORTEC 9315 photocounting system, under the control of a MINC 11 (DEC) minicomputer.

Results

A. Manganyl Porphyrins in Nonaqueous Solutions. We have explored different routes to manganyl complexes of tetramesitylporphyrin (TMP), the results of which are summarized in Scheme I. Electrochemical oxidation of $ClMn^{III}TMP$ (**1**) in acetonitrile containing 0.1 M tetrabutylammonium perchlorate (TBAP) and 0.04 M tetrabutylammonium hydroxide (TBA(OH)) at +0.6 V (vs. SCE) produced a red species, **5**, with an absorption spectrum characteristic of a Mn^{IV} porphyrin: the split Soret band found in **1** (478, 401, 372 nm) was replaced by a single Soret band at 418 nm. The spectrum of **5** is similar to that of the previously characterized species, **2**, prepared by oxidizing **1** with *m*-chloroperoxybenzoic acid (mCPBA) in the presence of 2 equiv of $(CH_3)_4NOH$. We find that electrochemical reduction of **2** in CH_2Cl_2 at +0.1 V quantitatively converted it to a species that was the same as **1**. Electrooxidation of this solution at +0.9 V regenerated the spectrum of **2** isosbestically. This redox cycling could be repeated several times without significant degradation.

When a solution of **1** in dry methylene chloride containing 0.1 M TBAP was cooled to −20 °C, electrooxidation at +1.20 V generated a green species, **4**, with a broad absorption band at 620 nm and decreased intensity in the Soret region (Figure 1), characteristic of porphyrin π-cation radical.[8a,19] That **4** was a one-electron oxidation product of **1** was demonstrated by spectrophotometric titration with tetrabutylammonium iodide, which showed isosbestic reconversion of the visible spectrum to that of **1**. Addition of TBA(OH) to the CH_2Cl_2 solution of **4** held at −20 °C immediately produced a red species, **3**, with an absorption spectrum characteristic of a Mn^{IV} porphyrin (Figure 1). Thus,

(20) Czernuszewicz, R. S.; Macor, K. A.; Kincaid, J. R.; Spiro, T. G., submitted for publication.

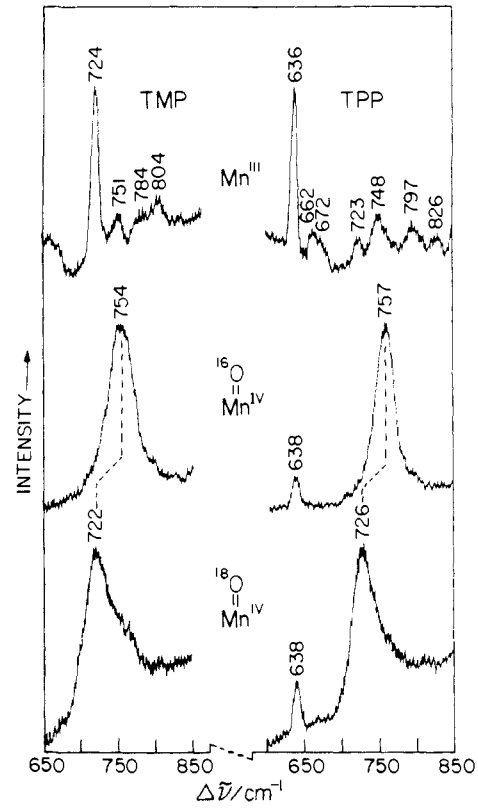

Figure 2. Resonance Raman spectra of $ClMn^{III}TMP$ (left panel) and $ClMn^{III}TPP$ (right panel) in CH_3CN (0.1 M TBAP) obtained before (top) and after electrooxidation at +0.6 V in the presence of TBA(^{16}OH) (middle) and TBA(^{18}OH) (bottom). All spectra were obtained in situ via backscattering from a controlled-potential bulk electrolysis Raman cell by using 4067 Å (~30 mW) Kr^+ ion laser excitation and 18 cm^{-1} slit widths.

Scheme I

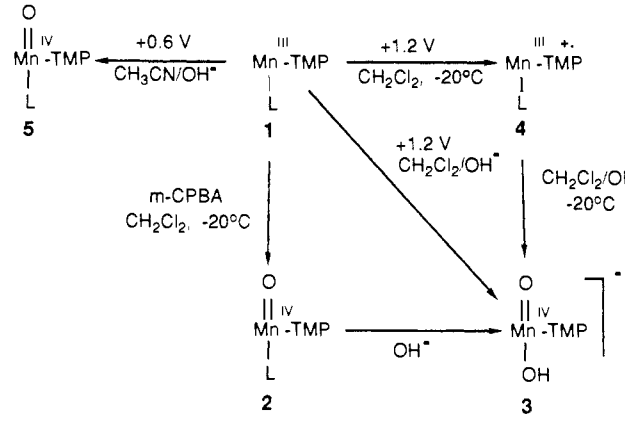

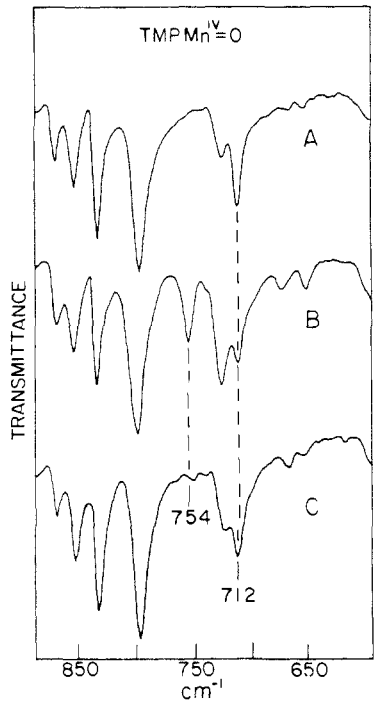

Figure 3. Infrared spectra (KBr pellets) of $(Mn^{IV}O)$TMP porphyrins isolated as solids: following (A) electrochemical oxidation of $ClMn^{III}$TMP (**1**) in CH_2Cl_2 (0.1 M TBAP) containing TBA(OH) at +1.2 V; (B) chemical oxidation of **1** in CH_2Cl_2 with mCPBA containing 2 equiv of $(CH_3)_4NOH$; (C) chemical oxidation as in part B followed by addition of excess TBA(OH).

generation of the oxo-Mn^{IV} porphyrin, instead of a Mn^{III} porphyrin π-cation radical, required the presence of a ligand (OH^-, mCPBA) capable of producing an oxo-manganese bond.

Direct evidence for this bond was obtained with RR spectroscopy. Figure 2 shows a portion of the RR spectrum of **5** generated with TBA(OH) (0.04 M) containing natural abundance OH^- and, alternatively, $^{18}OH^-$. The prominent band at 754 cm^{-1} which replaced a weak 751-cm^{-1} porphyrin band in the Mn^{III} spectrum is attributed to the stretching mode of the Mn–O bond, since it shifts to 722 cm^{-1} upon ^{18}O substitution; the expected shift for a Mn–O diatomic oscillator is 33 cm^{-1}. There was no shift when OD^- was used, indicating that the Mn-bound O atom is not protonated.

Tetramesitylporphyrin was used in these experiments to avoid complications that might arise from dimerization of the manganyl porphyrin, the mesityl substituents inhibiting dimerization via steric hindrance. μ-Oxo-Mn^{IV} porphyrins are known, and have been characterized crystallographically.[21] Manganyl porphyrins are therefore expected to condense to μ-oxo dimers at sufficiently high concentrations. We have found, however, that when $ClMn^{III}$TPP (TPP = tetraphenylporphyrin) and $ClMn^{III}$OEP (OEP = octaethylporphyrin) were electrooxidized under the conditions that produced **5** (+0.6 V in CH_3CN/0.1 M TBAP/0.04 M TBA(OH)), the same RR signatures of the Mn–O bond were obtained with ν_{MnO} = 757 (Figure 2) and 754 cm^{-1} (not shown), respectively. The concentration required for significant dimerization is not known, but Collman et al.[22] have noted anomalous kinetics in O atom transfer reactions involving MnTPP at higher concentrations and suggested dimerization of the presumed manganyl intermediate as a possible factor. Below ~1.0 mM the kinetics were first order in MnTPP, indicating that the intermediate remained monomeric. The concentration used for the RR experiment, 0.5 mM, falls in this range.

(21) (a) Smegal, J. A.; Schardt, B. C.; Hill, C. L. *J. Am. Chem. Soc.* **1983**, *105*, 3510–3515. (b) Schardt, B. L.; Hollander, F. J.; Hill, C. L. *J. Am. Chem. Soc.* **1982**, *104*, 3964–3972. (c) Smegal, J. A.; Hill, C. L. *J. Am. Chem. Soc.* **1983**, *105*, 3515–3521.

(22) Collman, J. P.; Brauman, J. I.; Meunier, B.; Hayashi, T.; Kodadek, T.; Raybuck, S. A. *J. Am. Chem. Soc.* **1985**, *107*, 2000–2005.

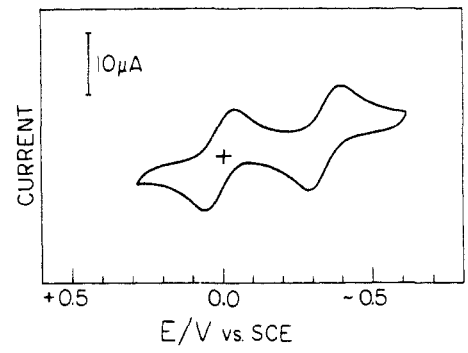

Figure 4. Cyclic voltammogram of $(AcO)Mn^{III}$TMPyP in 1 M NaOH at a glassy carbon electrode with 100 mV/s scan rate.

We were unable to obtain RR spectra of **2**, prepared by mCPBA oxidation of **1** in the presence of 2 equiv of $(CH_3)_4NOH$, due to high luminescence backgrounds, perhaps arising from trace degradation products. The IR spectrum of **2** (Figure 3, spectrum B), however, shows a band at 754 cm^{-1}, the same frequency as the ν_{MnO} RR band. Neither this band nor another one at 712 cm^{-1} is seen in the IR spectrum of **1** (not shown). When TBA(OH) was added to the solution of **2** in CH_2Cl_2, the 712-cm^{-1} band grew in intensity at the expense of the 754-cm^{-1} band (spectrum C). The IR spectrum (A) of **3**, prepared by electrooxidizing **1** in CH_2Cl_2/0.1 M TBAP containing excess TBA(OH), showed only the 712-cm^{-1} band. In the next section we demonstrate that the 712-cm^{-1} band is attributable to ν_{MnO} when there is a trans OH^- ligand. Thus $(Mn^{IV}O)$TMP in CH_2Cl_2 readily coordinates OH^-. The affinity is high enough that the ~1 mM OH^- present during mCPBA oxidation is sufficient to produce ~50% of the trans OH^- adduct. In CH_3CN, however, the presence of 40 mM TBA(OH), needed to form the manganyl species via electrooxidation, does not produce the trans OH^- adduct (adding larger amounts of hydroxide leads to decomposition of the Mn^{IV} species). Presumably OH^- affinity is lowered because CH_3CN solvates the manganyl porphyrin more effectively.

It is unclear whether CH_3CN actually ligates $(Mn^{IV}O)$TMP, however, because ν_{MnO} = 754 cm^{-1} for the species lacking trans OH^-, whether the solvent is CH_3CN or CH_2Cl_2. A downshift of ν_{MO} is expected upon trans ligand coordination to an oxo–metal bond, as documented for several adducts of vanadyl porphyrins.[23] There was no evidence for CH_3CN ligation of the vanadyl group. On the other hand the downshift becomes progressively smaller with decreasing donor strength of the axial ligand. Consequently the effect of a CH_3CN ligand might be quite small. In any event ν = 754 cm^{-1} is a reasonable estimate for the Mn–O frequency in five-coordinate manganyl TMP and OEP. The slight upshift to 757 cm^{-1} in $(Mn^{IV}O)$TPP is attributable to the enhanced electron withdrawing tendency of the phenyl, relative to the ethyl and mesityl substituents,[23] as discussed in connection with the comparison of (VO)OEP and (VO)TPP.[23]

B. Manganyl TMPyP in Aqueous Alkali. When AcO-Mn^{III}TMPyP (AcO = acetate, TMPyP = tetrakis(methylpyridinium)porphyrin) was dissolved in 1 M NaOH, cyclic voltammetry at a glassy carbon electrode (Figure 4) showed cleanly reversible one-electron reduction and oxidation processes at –0.32 and +0.02 V versus SCE, respectively. The absorption spectrum of the electrooxidized solution is characteristic of a Mn^{IV} porphyrin, with a Soret maximum at ~450 nm (Figure 5). These observations are consistent with those of Harriman and Porter on the same system.[24]

Figure 6 shows Raman spectra in the 300–900-cm^{-1} region for the Mn^{III} species excited at 457.9 nm, in resonance with the Soret absorption band. In addition to several porphyrin skeletal modes, a broad band is seen at 495 cm^{-1}, which shifts down to 481 cm^{-1}

(23) Su, Y. O.; Czernuszewicz, R. S.; Miller, L. A.; Spiro, T. G. *J. Am. Chem. Soc.*, preceding paper in this issue.

(24) Harriman, A.; Porter, G. *J. Chem. Soc., Faraday Trans. II* **1979**, *75*, 1532–1542.

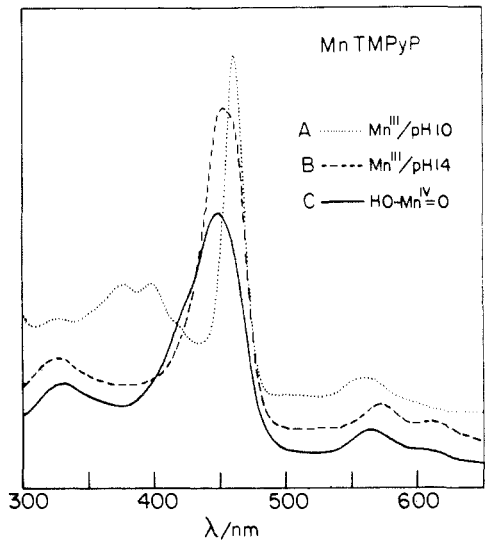

Figure 5. Electronic absorption spectra of MnTMPyP porphyrins in aqueous solutions: (A) $Mn^{III}TMPyP$, pH 10 (λ_{max} = 327, 376, 398, 462, 560, 594 nm); (B) $(HO)_2Mn^{III}TMPyP$, pH 14 (λ_{max} = 327, 452, 458, 573, 610 nm); (C) $(HOMn^{IV}O)TMPyP$, pH 14 generated by electrooxidation of (B) at +0.5 V (λ_{max} = 332, 436 sh, 449, 563, 606 nm).

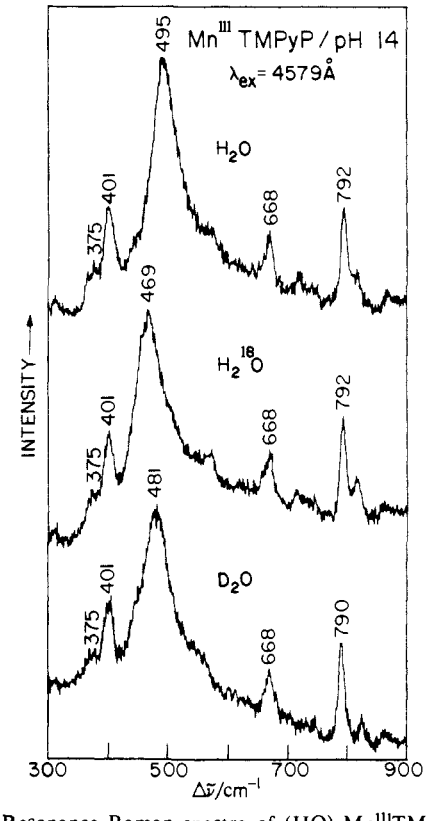

Figure 6. Resonance Raman spectra of $(HO)_2Mn^{III}TMPyP$ in 1 M NaOH (top), 1 M $Na^{18}OH$ (middle), and 1 M NaOD (bottom) aqueous solution. All spectra were obtained via backscattering from spinning NMR tubes by using 4579 Å Ar^+ ion laser excitation (~50 mW) and 6 cm^{-1} slit widths.

when the solution is prepared in D_2O and to 469 cm^{-1} in $H_2{}^{18}O$. This band is assigned to the symmetric $Mn^{III}(OH)_2$ stretching mode of a *trans*-dihydroxide complex. A triatomic oscillator calculation with point mass (17 amu) OH ligands reproduces this frequency with a symmetric stretching force constant of 2.46 mdyn/Å and predicts D_2O and $H_2{}^{18}O$ shifts (point mass 18 and 19 ligands) of 14 and 27 cm^{-1}, in excellent agreement with experiment. If instead a Mn–OH diatomic oscillator is assumed, modelling a 5-coordinate complex, then the required force constant is 1.87 mdyn/Å and the predicted D_2O and $H_2{}^{18}O$ shifts are 10

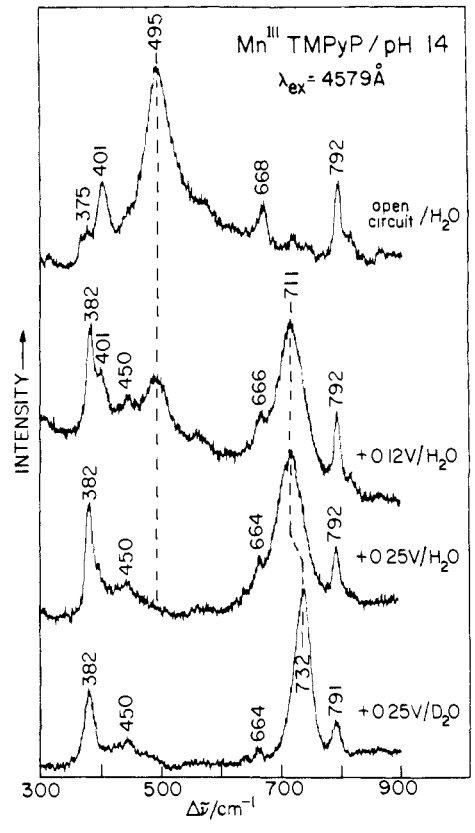

Figure 7. Resonance Raman spectra of manganese TMPyP in 1 M NaOH (top three) and 1 M NaOD (bottom) at various oxidation potentials. All spectra were obtained in situ via backscattering from a controlled-potential bulk electrolysis Raman cell by using 4579 Å Ar^+ ion laser excitation (~50 mW) and 6 cm^{-1} slit widths.

and 20 cm^{-1}, significantly smaller than observed. Thus, a *trans*-dihydroxo complex is indicated by the vibrational data. The breadth of the 495-cm^{-1} band suggests that the OH ligands are strongly H-bonded to sovlent H_2O molecules. It is interesting that the characteristic Mn^{III} split Soret band seen at pH 10 collapses to a single (broad) Soret band at pH 14 (see Figure 5). The Mn^{III} Soret band splitting has been attributed[25] to mixing of the porphyrin π–π^* transitions with a nearby Mn d_π–porphyrin π^* charge-transfer transition. We infer that this mixing is diminished in the *trans*-dihydroxide complex because the energy of the charge-transfer transition is lowered via the OH^- π–Mn d_π interaction.

Figure 7 shows RR spectra in the same frequency region for solutions held at successively higher potentials. As the potential was raised through the Mn^{IV}/Mn^{III} redox potential, the 495-cm^{-1} band is replaced by an equally broad band at 711 cm^{-1}, which shifts down to 684 cm^{-1} in $H_2{}^{18}O$ (not shown). This band is assigned to ν_{MnO} of the electrogenerated manganyl porphyrin. It is at the same frequency seen in the IR spectra (Figure 3) of $(Mn^{IV}O)TMP$ in CH_2Cl_2 containing excess OH^-.

Proof that this band is associated with a trans OH^- adduct is provided by the remarkable 21-cm^{-1} *upshift* in D_2O (Figure 7, bottom). Although some sensitivity to D_2O associated with H-bond differences might be expected, the upshift is much too large to be attributed to a difference in D- versus H-bonding. It must instead reflect differential coupling with an internal coordinate involving H or D atoms. The only plausible coupling scheme is one involving the Mn–O–H bending coordinate of a trans axial OH^- ligand. The frequencies of Mn–O–H bending modes are variable, but they can be in the ~700-cm^{-1} range for strongly H-bonded OH groups.[26] If the natural frequency for

(25) Gouterman, G. In *The Porphyrins*; Dolphin, D., Ed.; Academic: New York, 1979; Vol. 3, pp 1–165.
(26) (a) Tarte, P. *Spectrochim. Acta* **1958**, *13*, 107–119. (b) Bulliner, P. A.; Spiro, T. G. *Inorg. Chem.* **1969**, *8*, 1023–1025.

Table I. Normal Mode Calculations for a HO-Mn=O Model[a]

mode character	ν (cm^{-1}) obsd	calcd	PED (%)[b] ν_{MnO}	ν_{MnOH}	δ_{MnOH}	ν_{OH}
		$H^{16}O$—Mn=^{16}O				
$\nu_{Mn^{16}O}$	711	710	75	9	16	
$\nu_{Mn^{16}OH}$		534	18	74	8	
$\delta_{Mn^{16}OH}$		785	7	17	76	
$\nu^{16}OH$		3591				100
		$H^{18}O$—Mn=^{18}O				
$\nu_{Mn^{18}O}$	684	686	75	14	10	
$\nu_{Mn^{18}OH}$		508	21	73	5	
$\delta_{Mn^{18}OH}$		774	4	12	84	
$\nu^{18}OH$		3579				100
		$D^{16}O$—Mn=^{16}O				
$\nu_{Mn^{16}O}$	732	731	64	30	5	
$\nu_{Mn^{16}OD}$		475	30	45	25	
$\delta_{Mn^{16}OD}$		620	6	24	70	
$\nu^{16}OD$		2623				100

[a] Only the modes in the Mn-O-H plane were calculated. The assumed geometry was Mn=O = 1.85 Å, Mn-OH = 2.00 Å, OH = 1.00 Å, ∠O-Mn=O = 180°, ∠Mn-O-H = 105°. The following force constants (mdyn/Å) were used: K_{MnO} = 3.43, K_{MnOH} = 2.6, K_{OH} = 7.2, and K_{MnOH} = 0.3. $H_{O\text{-}Mn=O}$ was set equal to zero, for convenience; the stretching frequencies are not affected by its magnitude. [b] Potential energy distribution (PED); % contributions from the indicated internal coordinates.

the postulated trans axial OH group were ~750 cm^{-1}, it could depress the Mn=O stretching frequency by a near resonant interaction. This interaction would be relieved in D_2O because of the large drop in the Mn-O-D frequency, resulting in a rise of the Mn=O frequency. We are able to calculate the observed 21-cm^{-1} upshift with a four-atom H—O—Mn=O model using reasonable force constants and structure parameters, as given in Table I. This calculation predicts the correct ^{18}O frequency shift and lends considerable confidence in the proposed trans HO—Mn=O structure. The model also predicts a Mn-OH stretching frequency at 533 cm^{-1}. This is not observed in the RR spectrum, presumably because of insufficient resonance enhancement.[23] Shiemke et al.[27] have recently invoked coupling of Fe-O-Fe stretching with Fe-O-D bending to explain complex D_2O effects on the RR spectrum of hemerythrin. The ν_{MnO} band is significantly broader in H_2O than in D_2O (Figure 7). This broadening may be associated with very rapid interconversion of the degenerate structures HO—Mn=O ⇄ O=Mn—OH via proton transfer to and from solvent, as also suggested for the analogous HO—V=O complex.[23] The rate might decrease sufficiently in D_2O to produce the observed narrowing.

Conversion of Mn^{III} to Mn^{IV}TMPyP also leads to the replacement of a porphyrin RR band at 401 cm^{-1} with another at 382 cm^{-1}; other porphyrin bands at 668 and 792 cm^{-1} are only slightly affected. The 401/382-cm^{-1} band corresponds to the ~390-cm^{-1} band of metallo TPP's, which is known to be sensitive to oxidation and spin state in iron TPP's.[28] It is curious that the frequency decreases upon oxidation, since an increase would have been expected on the iron TPP analogy.

Figure 8 shows the X-band EPR spectrum of the (HO-Mn^{IV}O)TMPyP complex at pH 14. Very similar spectra have been obtained for the (Mn^{IV}O)TMP species **5**, **2**, and **3**, and for (Mn^{IV}O)TPP. The strong broad resonance at $g_\perp \sim 4.0$ and the weak signal at $g_\parallel \sim 2.0$ are similar to those observed for other high-spin ($s = {}^3/_2$) monomeric Mn^{IV} species.[8b,29] The anisotropy in the resonances has been attributed for other d^3 ions to an axial symmetry field with a large value for the zero-field splitting parameter, D.[6,30] We note, however, that the EPR spectra reported by Schappacher and Weiss[8e] for Mn^{IV} porphyrins containing

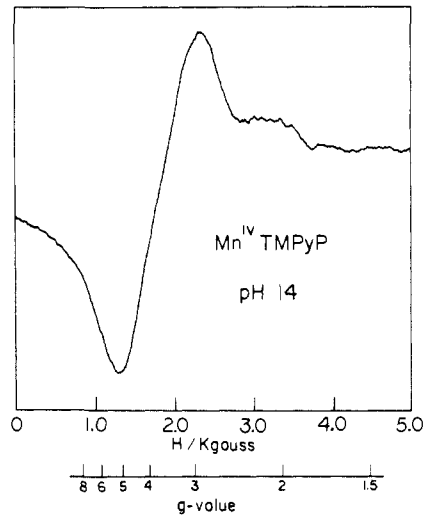

Figure 8. First derivative EPR spectrum (120 K) of electrooxidized Mn^{III}TMPyP at pH 14. Spectrometer settings: 100 kHz modulation frequency, 2.5 × 10 modulation amplitude, 8.0 × 10^2 receiver gain, 10 mW microwave power, 9.03 GHz microwave frequency, and 4 min scan time.

phenyl or pentafluorophenyl substituents differ significantly in having a weak $g_\parallel = 4.0$ and strong $g_\perp = 2.0$ signal. The axial ligation has not been characterized in this case. Whether the altered oxidation procedure or different axial ligation can account for the difference is unclear. Dimeric μ-oxo-manganese^{IV} porphyrins have been shown to be EPR silent due to antiferromagnetic coupling between the d^3 ions.[21a]

Harriman and Porter[24] observed absorption spectral changes for Mn^{IV}TMPyP at lower pH values which they interpreted as a protonation step with a pK_a of ~10.7. We attempted RR spectroscopy on lower pH solutions in hopes of characterizing the protonation product, expected to be $(HO)_2Mn^{IV}$TMPyP, but without success. Electrooxidation in a pH 12.5 solution at +0.6 V led to a RR spectrum containing 495- and 711-cm^{-1} bands of comparable intensity, indicating a ~50:50 mixture of (HO)-(Mn^{IV}O)TMPyP and $[(HO)_2Mn^{III}TMPyP]^-$. Prolonged electrolysis led to a diminution of the Mn^{IV} signal, and a substantial lowering of the pH, indicating consumption of hydroxide. We conclude that the putative $(HO)_2Mn^{IV}$TMPyP is unstable with respect to an irreversible reaction which regenerates the Mn^{III} species and consumes OH^-. The oxidation product of this intriguing reaction has not yet been identified. The irreversibility of the system means that the spectrophotometrically estimated pK_a of 10.7 cannot be relied on.

Discussion

The characterization of the Mn-O bond of manganyl porphyrins by vibrational spectroscopy described here provides new insight into the electronic basis for the reactivity of oxometal porphyrins. A particularly revealing comparison is provided by oxo adducts of the four adjacent members of the third-row transition-metal ions V^{IV}, Cr^{IV}, Mn^{IV}, and Fe^{IV}. Vanadyl and chromyl porphyrins are stable entities, while manganyl and ferryl decompose readily. This reactivity trend correlates directly with the M-O bond strength as revealed by the M-O stretching frequencies. It has been known that $\nu_{M\text{-}O}$ is ~1000 cm^{-1} for both $V^{IV}O$[23] and $Cr^{IV}O$ porphyrins[7c] but ~800 cm^{-1} for $Fe^{IV}O$ porphyrins.[15g,h,l] It might have been thought that the stretching frequency for $Mn^{IV}O$ porphyrins would occupy an intermediate position. The present work shows, however, that ν_{MnO} is significantly lower even than ν_{FeO}. In making quantitative comparisons of this type it is important to control the axial ligation, porphyrin type, and to some extent even the solvent, all of which have been shown to influence the M-O stretching frequency.[23] Table II compares frequencies for the unligated, five-coordinate oxometal TPP's. Also given are force constants calculated on the diatomic oscillator approximation. This approximation is reasonable since coupling of M-O stretching

(27) Shiemke, A. K.; Loehr, T. M.; Sanders-Loehr, J. *J. Am. Chem. Soc.* **1986**, *108*, 2437-2443.
(28) Burke, J. M.; Kincaid, J. R.; Spiro, T. G. *J. Am. Chem. Soc.* **1978**, *100*, 6077-6083.
(29) Camenzind, M. J.; Hollander, F. J.; Hill, C. L. *Inorg. Chem.* **1983**, *22*, 3776-3784.

Table II. Resonance Raman M=O Stretching Frequencies (cm^{-1}) for First Transition Row Metalloporphyrins in 5-Coordinate and 6-Coordinate *trans*-Deuterio Forms

	5-coordinate	K_{MO}[a] (mdyn/Å)	6-coord	K_{MO}[b] (mdyn/Å)	electron count
V^{IV}	1007[c]	7.26	895[d]	5.50	d^1
Cr^{IV}	1025[e]	7.58			d^2
Mn^{IV}	754[f]	4.15	732[g]	3.43	d^3
Fe^{IV}	843[h]	5.21			d^4

[a] Calculated for a diatomic oscillator. [b] Calculated for a HO—M=O model, with parameters as in Table I, allowing K_{MO} to fit the observed frequency. [c] ($V^{IV}O$)TPP in hexane.[23] [d] ($V^{IV}O$)TMPyP in 1 M NaOH.[23] [e] ($Cr^{IV}O$)TPP in KBr pellet (infrared).[7c] [f] ($Mn^{IV}O$)TPP and ($Mn^{IV}O$)TMP in CH_3CN (this work). [g] ($Mn^{IV}O$)TMPyP in 1 M NaOH (this work). [h] ($Fe^{IV}O$)TMP in toluene.[15l]

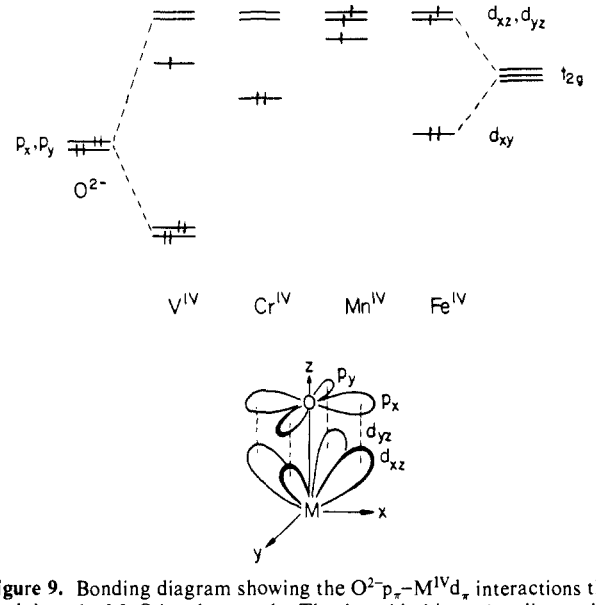

Figure 9. Bonding diagram showing the $O^{2-}p_\pi$–$M^{IV}d_\pi$ interactions that modulate the M–O bond strength. The d_{xy} orbital is nonbonding and its energy decreases with increasing effective nuclear charge from V^{IV} to Fe^{IV}, with the exception of Mn^{IV}, where it is brought close to d_{xy},d_{yz} by the exchange interactions in the high-spin half-filled t_{2g} subshell.

with the nearly orthogonal internal coordinates of the porphyrin is expected to be small, and in any event essentially the same for all the species. The force constants correct for the slight effect on the frequencies of the changing metal mass.

The variation among these force constants is very far from monotonic. There is a slight increase from V^{IV} to Cr^{IV}, a very large decrease to Mn^{IV}, and a substantial increase again to Fe^{IV}. We offer an explanation of this peculiar pattern in terms of the d electron count and the special properties of the half-filled t_{2g}^3 subshell. Figure 9 provides a qualitative bonding diagram. The O^{2-} ligand donates both σ (omitted from the diagram) and π electrons to the M^{4+} ions. The filled p orbitals of the ligand (p_x and p_y, with z as the M–O direction) interact with the d_π orbitals (d_{xz},d_{yz}), which become antibonding. The d_{z^2} and $d_{x^2-y^2}$ orbitals are σ-antibonding with respect to the M–O bond and the M–N porphyrin bonds, respectively, and are at much higher energy. The d_{xy} orbital is nonbonding. This orbital accommodates the single d electron of V^{IV}, allowing unimpeded O → M π interactions. Since there are two π orbital overlaps, the result is formally a M≡O triple bond. The high bond order is reflected in the elevated force constant, 7.25 mdyn/Å. This formulation holds as well for Cr^{IV}. The Cr^{IV}≡O force constant is slightly higher, 7.58 mdyn/Å due to the higher effective nuclear charge of Cr^{IV} relative to V^{IV}. The short Cr–O bond length (1.57 Å) is consistent with this interpretation.[7c] The separation between d_{xy} and d_{xz},d_{yz} is sufficiently large that both Cr^{IV} valence electrons are forced into the d_{xy} orbital, resulting in a low-spin configuration.[7c] For Fe^{IV} (d^4), the two extra electrons must enter the π-antibonding d_{xz} and d_{yz} orbitals, reducing the bond order by one unit to M=O. This is reflected in the 31% decrease in the force constant, to 5.21 mdyn/Å.

If the same d orbital pattern were to hold for Mn^{IV}, we might expect the Mn–O force constant to be intermediate between Cr^{IV} and Fe^{IV}, with two electrons filling the d_{xy} orbital, and one electron in the pair of two d_π orbitals; the M–O bond order would be 2.5, and the stretching frequency would have an intermediate value. The EPR spectrum, however, shows three unpaired electrons, not one. The reason for the high-spin configuration must be the special stability, due to exchange interactions, of the half-filled t_{2g} (in O_h symmetry) subshell. This stabilization of the high-spin d^3 configuration effectively brings the d_{xy} orbital energy close to those of d_{xz} and d_{yz}. The latter remain π-antibonding with respect to the oxo ligand, however, and the M–O order is 2 as it is for Fe^{IV}.

We attribute the fact that the M–O bond order is substantially lower for Mn^{IV} than for Fe^{IV} primarily to the higher effective nuclear charge on Fe^{IV} relative to Mn^{IV}, and its consequences for the orbital energies. While the V^{IV}/Cr^{IV} comparison gives only a 5% effect for a unit increase in nuclear charge, the Mn^{IV}/Fe^{IV} difference is expected to be greater because the M=O bond is weaker and more polarizable than the M≡O bond; by extension, the M=O bond is more susceptible to porphyrin π delocalization. Striking evidence for a porphyrin effect is provided by the position of the β-pyrrole proton magnetic resonance for five-coordinate ($M^{IV}O$)TMP complexes, −35 ppm for Mn^{IV} [30] but +8.5 ppm for Fe^{IV}.[31] The upfield shift seen for Mn^{IV} indicates appreciable porphyrin → d_π donation,[32] which is evidently inhibited for Fe^{IV}. This difference is fully consistent with weaker O^{2-} → d_π donation for Mn^{IV} than for Fe^{IV}. While the orbital energies and overlaps are difficult to quantify, it seems apparent that the increased nuclear charge on Fe^{IV} brings its d_π orbitals into better alignment with the O^{2-} p_π orbitals and poorer alignment with the porphyrin donor orbitals (probably the filled $3e_u$ orbital, mainly[32]) than is the case for Mn^{IV}.

When trans ligands are bound to the $M^{IV}O$ unit, the M–O frequency and force constant decreases, because the donor properties of the ligand counteract the donor interactions from O^{2-}.[23] The strongest effect is shown by OH^-, which is a good π as well as σ donor, and competes most effectively with O^{2-}. Table II also compares Mn–O frequencies and force constants for DO–M–O complexes of V^{IV} and Mn^{IV}. The comparison is made for the OD^- rather than the OH^- complex in which the M–O frequency is depressed by the special coupling with the Mn–O–H bend; this coupling is relieved in the OD^- complex. The frequency decrease, relative to the five-coordinate value, is much smaller for Mn^{IV} (21 cm^{-1}) than V^{IV} (110 cm^{-1}), but this is due largely to the stronger coupling with the M^{IV}–OD stretch whose frequency is closer to ν_{M-O} for Mn^{IV} than V^{IV} (Table I). The change in force constant is substantial in both cases but is somewhat less for Mn^{IV} (17%) than V^{IV} (24%).

The weakness of the Mn^{IV}–O bond is expected to enhance the basicity of the oxo ligand. Harriman and Porter[24] have estimated its pK_a at 10.7 from absorption spectral changes, but, as noted in the previous section, this estimate is unlikely to be reliable in view of the evidence for irreversible decomposition accompanying protonation. Nevertheless, the decomposition reaction emphasizes the proton affinity of the oxo ligand.

The Mn^{IV}–O proton affinity is further emphasized by the report of Makino et al.[15k] that when Mn is substituted for Fe in horseradish peroxidase (HRP), the compound II intermediate of the peroxide reaction contains Mn^{IV}—OH rather than Mn^{IV}=O. A RR band at 623 cm^{-1} shifted to 596 cm^{-1} when the intermediate was prepared with $H_2{}^{18}O_2$, rather than $H_2{}^{16}O_2$, and it shifted to 613 cm^{-1} when the reaction was carried out in D_2O. This result confirmed a previous inference from proton NMR relaxation measurements showing a rapidly exchanging paramagnetically relaxed proton at a distance consistent with Mn–OH.[3b,33] In

(30) Groves, J. T.; Stern, M. K. *J. Am. Chem. Soc.* **1987**, *109*, 3812–3814.
(31) Balch, A. L.; Chan, Y.-W.; Cheng, R.-J.; La Mar, G. N.; Latos-Grazynski, L.; Renner, M. W. *J. Am. Chem. Soc.* **1984**, *106*, 7779–7785.
(32) Goff, H. M. In *Iron Porphyrins*; Part One; Lever, A. B. P., Gray, H. B., Eds.; Addison-Wesley: Reading, MA, 1983; pp 250–254.

compound II the Fe-containing protein ν_{FeO} is at ~788 cm^{-1}, consistent with a Fe=O bond trans to a strongly H-bonded imidazole ligand.[15b] At pH values below 8.5 the frequency shifts down ~13 cm^{-1}. This effect has been attributed to H-bonding from a protonatable distal residue, probably histidine.[15c] Thus in compound II the distal proton resides on an adjacent protein residue when the M-O bond contains Fe^{IV}, but on the oxo ligand (perhaps with a reverse H-bond interaction to the same distal ligand) when it contains Mn^{IV}. The 623-cm^{-1} Mn-HRP II RR peak is unaltered between pH 7 and 10, indicating the distal proton to be much more tightly held in the Mn protein.

Finally, it is worth remarking on the implications of the present results with respect to the reactivity patterns of manganyl and ferryl porphyrins. Oxomanganese(V) porphyrins and oxoiron(IV) porphyrin cation radicals are powerful oxidants capable of alkane hydroxylation and olefin epoxidation even at low temperatures.[8a,17] Other things being equal, manganese(III) should be easier to oxidize than iron(III). Indeed, manganyl(IV) porphyrins are relatively stable; in this study they have been characterized at room temperature. Ferryl(IV) porphyrins have limited stability, however, and have been characterized only at low temperature.[2] To the extent that the π-bond order is lower for Mn^{IV}=O than for Fe^{IV}=O, the oxygen atom of the former should both be less electrophilic and have less unpaired electron density than the latter. Consistent with this notion we find that electrochemically generated ferryl(IV) porphyrins *do* epoxidize olefins at room temperature but with an uncharacteristic *loss* of olefin configuration,[34] just as manganese(IV) porphyrins do.[8b]

This weakness of the Mn^{IV}=O bond may help account for why nature has chosen manganese for the O_2 generating apparatus of green plants, The water oxidation center associated with the chloroplast photosystem contains a cluster of manganese ions whose oxidation level is intimately associated with O_2 production.[35] It is believed that the Mn ions shuttle between the Mn^{III} and Mn^{IV} oxidation levels.[36] While the Mn ions are not imbedded in porphyrins, the present inference about the weakness of the Mn^{IV}=O bond is not limited to porphyrins. Rather it is associated with the electronic properties of the d^3 ions; oxidation of Mn^{III}-bound water, accompanied by proton transfer, should generally lead to weak Mn^{IV}=O bond formation. Two Mn^{IV}=O units in the proper orientation could readily generate Mn^{III}-O-O-Mn^{III}, and then O_2 via electron transfer, perhaps from other Mn ions in the cluster.[37]

Acknowledgment. This work was supported by U.S. Department of Energy Grant DE-AC02-81ER10861 (to T.G.S.) and National Science Foundation Grant CHE 8706310 (to J.T.G.). We thank Prof. Harold Goff for helpful discussions.

Registry No. 1, 85939-49-7; **2**, 104025-51-6; **3**, 108535-08-6; **4**, 104025-52-7; 6, 114300-80-0; $ClMn^{III}OEP$, 28265-17-0; $ClMn^{III}TPP$, 32195-55-4; $ClMn^{III}TMPyP$, 97057-20-0; $(AcO)Mn^{III}TMPyP$, 114324-35-5; $(Mn^{IV}O)TPP$, 76077-77-5; $[(HO)_2Mn^{III}TMPyP]^-$, 89043-43-6.

(33) (a) Ferrante, R. F.; Wilkerson, J. L.; Graham, W. R. M.; Weltner, W. *J. Chem. Phys.* **1977**, *67*, 5904. (b) Richens, D. T.; Sawyer, D. T. *J. Am. Chem. Soc.* **1979**, *101*, 3681-3683. (c) Morishima, I.; Ogawa, S. *Biochemistry* **1978**, *17*, 4384-4388.

(34) Groves, J. T.; Stern, M. K., presented at the Third Chemical Congress of North America, Toronto, June 1988.

(35) Dismukes, G. C.; Siderer, Y. *Proc. Natl. Acad. Sci. U.S.A.* **1981**, *78*, 274-278.

(36) (a) Dismukes, G. C.; Fems, K.; Watnick, P. *Photobiochem. Photobiophys.* **1982**, *3*, 243-256. (b) Dismukes, G. C. *Photochem. Photobiol.* **1986**, *43*, 99-115.

(37) (a) Renger, G. In *Photosynthetic Oxygen Evolution*; Metzner, H., Ed.; Academic: London, 1978; pp 239-248. (b) Radner, R.; Olligner, O. *FEBS Lett.* **1986**, *195*, 285-289.

Differences between Human and Porcine Insulin Investigated by Linear Prediction Carbon-13 NMR

Jens J. Led,*,† Henrik Gesmar,† Kim R. Hejnaes,‡ and Finn B. Hansen‡

Contribution from the Department of Chemical Physics, University of Copenhagen, The H. C. Ørsted Institute, Universitetsparken 5, DK-2100 Copenhagen Ø, Denmark, and Nordisk Gentofte, Niels Steensensvej 1, DK-2820 Gentofte, Denmark. *Received September 21, 1987*

Abstract: The linear prediction method was used to analyze the ^{13}C NMR free induction decay signals of a series of insulins and insulin derivatives. The higher resolution provided by this method, as compared with the conventional Fourier transformation approach, revealed differences between the ^{13}C NMR spectra of human and porcine insulins. This may indicate differences between the structures of these closely related proteins beyond the difference between their primary structures. Such differences have not been observed previously either in solution or in the crystal phase.

The function of biologically active proteins depends on even small differences and changes in their solution structures. This emphasizes the importance of methods by which such structural variations can be detected. In general, NMR spectroscopy is suitable for that purpose. Thus, by a variety of techniques,[1,2] information about structural and kinetic details of proteins has been obtained from the ^1H NMR signals of characteristic groups in the molecules. Furthermore, with the introduction of two-dimensional (2D) experiments, NMR spectroscopy has become the first technique by which the overall three-dimensional structure of small proteins in solution can be determined.[3-5] So far, these techniques have almost exclusively been based upon the Fourier transform (FT) of the time-domain NMR signal—or the free induction decay (FID). Recently it was demonstrated[6] that linear prediction (LP) analyses of the ^1H and ^{13}C FID's of peptides and small proteins are feasible, yielding quantitative spectral infor-

† The H. C. Ørsted Institute.
‡ Nordisk Gentofte.

(1) Jardetsky, O.; Roberts, G. C. K. *NMR in Molecular Biology*; Academic: New York, 1981.

(2) Fox, R. O.; Evans, P. A.; Dobson, C. M. *Nature (London)* **1986**, *320*, 192-194.

(3) Wagner, G.; Wüthrich, K. *J. Mol. Biol.* **1982**, *155*, 347-366.

(4) Zuiderweg, E. R. P.; Scheek, R. M.; Boelens, R.; van Gunsteren, W. F.; Kaptein, R. *Biochimie* **1985**, *67*, 707-715.

(5) Kline, A. D.; Braun, W.; Wüthrich, K. *J. Mol. Biol.* **1986**, *189*, 377-382.

(6) Gesmar, H.; Led, J. J. *J. Magn. Reson.* **1988**, *76*, 183-192.

0002-7863/88/1510-4165$01.50/0